THE JOURNAL OF BIOLOGICAL CHEMISTRY VOL. 290, NO. 10, pp. 6397–6407, March 6, 2015


# β-Spectrin Regulates the Hippo Signaling Pathway and Modulates the Basal Actin Network*[S]

Received for publication, December 4, 2014, and in revised form, January 12, 2015 Published, JBC Papers in Press, January 14, 2015, DOI 10.1074/jbc.M114.629493

**Kenneth Kin Lam Wong[‡§], Wenyang Li[¶], Yanru An[‡§], Yangyang Duan[‡], Zhuoheng Li[‡], Yibin Kang[¶], and Yan Yan[‡§1]**

*From the [‡]Division of Life Science and [§]Center of Systems Biology and Human Health, School of Science and Institute for Advanced Study, Hong Kong University of Science and Technology, Clear Water Bay, Kowloon, Hong Kong, China and the [¶]Department of Molecular Biology, Princeton University, Princeton, New Jersey 08544*

**Background:** The Hippo signaling pathway is regulated by mechanical signals from the cytoskeleton.
**Results:** Perturbation of the spectrin cytoskeleton lead to loss of Hippo signaling phenotypes in *Drosophila* and mammalian cells.
**Conclusion:** β-Spectrin regulates Hippo signaling activity in *Drosophila* and mammalian cells.
**Significance:** The spectrin cytoskeleton can function as a tension-sensing system and feed into the Hippo pathway.

**Emerging evidence suggests functional regulation of the Hippo pathway by the actin cytoskeleton, although the detailed molecular mechanism remains incomplete. In a genetic screen, we identified a requirement for β-Spectrin in the posterior follicle cells for the oocyte repolarization process during *Drosophila* mid-oogenesis. *β-spectrin* mutations lead to loss of Hippo signaling activity in the follicle cells. A similar reduction of Hippo signaling activity was observed after β-Spectrin knockdown in mammalian cells. We further demonstrated that *β-spectrin* mutations disrupt the basal actin network in follicle cells. The abnormal stress fiber-like actin structure on the basal side of follicle cells provides a likely link between the *β-spectrin* mutations and the loss of the Hippo signaling activity phenotype.**

The evolutionarily conserved Hippo signaling pathway has been discovered to have an essential function in organ size control (1). It was later found to also play important roles in processes such as differentiation and morphogenesis in various developmental contexts (1–3). The upstream regulatory network of the Hippo pathway is complex in contrast to its well defined core pathway components (2). Importantly, multiple lines of evidence have pointed to the actin cytoskeleton as an essential regulator of Hippo signaling activity (4–10). These observations are consistent with the hypothesis that cells in tissues and organs can sense mechanical signals such as geometry and tension and that these mechanical signals are passed through the actin cytoskeleton to the Hippo pathway for coordination of cell behaviors. However, the mechanistic link between the actin cytoskeleton and the Hippo pathway remains largely unclear.

Here we identify a novel function of β-Spectrin, an actin cross-linking protein (11–13), in the Hippo signaling pathway. Spectrins, originally identified from human erythrocyte ghosts in 1968 (14), are filamentous proteins that are organized into a polygonal meshwork underneath the red blood cell membrane (15, 16). The spectrin-based cytoskeleton confers high deformability and elasticity to the cell membrane for red blood cells to endure the mechanical and osmotic stresses as they circulate through the body. Defects in the spectrin network are associated with many forms of hemolytic anemia (17–20). The spectrin cytoskeletal network exists in most metazoan cell types (21–24), where it has been found to be important for the formation of cell membrane microdomains (25–28), axonal growth (29, 30), and synapse development (31–34). Although spectrins exhibit diverse functions in different tissues and organs, the spectrin network seems to have a general structural and supporting function related to the mechanical properties of cells (24, 35). A recent study has demonstrated that the spectrin cytoskeleton in the *Caenorhabditis elegans* touch sensory neurons is required for maintaining neuronal prestress status, protecting these neurons from mechanical stress, and enhancing the mechanical sensitivity of these neurons (36).

In this study, we demonstrate that *β-spectrin* mutations disrupt Hippo signaling activity in the follicular epithelial cells during *Drosophila* oogenesis. We also show that the requirement of β-Spectrin in the Hippo signaling pathway is conserved in mammalian cells. Although the link between actin stress fibers and YAP/TAZ activity has been established previously in mammalian cell cultures (4–6, 9), here we are able to demonstrate a link between the formation of abnormal stress fibers and loss of Hippo signaling activity in *β-spectrin* mutant cells in an *in vivo* developmental context.

## EXPERIMENTAL PROCEDURES

*Fly Strains—β-spectrin* alleles were isolated from a genetic mosaic screen described previously (37). The following fly strains were used: Kinesin-β-gal (38), Staufen-GFP (39), *mirror-lacZ* (40), *kekkon-lacZ* (41), *expanded-lacZ* (42), *diap1-lacZ* (43), E-cadherin-GFP (44), and Utrophin-GFP (45). Fly lines for mapping, *traffic jam-Gal4 (tj-Gal4)*, *nubbin-Gal4 (nub-Gal4)*, and transgenic UAS-RNAi lines, including *EGFP RNAi*, *α-spectrin RNAi*, *mer RNAi*, and *yki RNAi*, were obtained from the Bloomington

* This work was supported by Research Grants Council of the Hong Kong Special Administrative Region Grants 16103314, AoE/M-09/12, and IGN12SC01.
[S] This article contains supplemental Movies 1 and 2.
[1] To whom correspondence should be addressed: Div. of Life Science, Center of Systems Biology and Human Health, Hong Kong University of Science and Technology, Clear Water Bay, Hong Kong, China. Tel.: 852-23585929; E-mail: yany@ust.hk.

Stock Center. Mosaic clones in the ovarian follicle cells and imaginal disc cells were generated using the FRT/FLP (flippase/flippase recognition target) system.

*Mutation Mapping*—The *FY18* complementation group was mapped through recombination mapping to the region proximal of *forked (f)* at 15F4-F7. Duplication mapping showed that the *FY18* complementation group could be rescued by Dp (1;Y)w73, which further narrowed the mutations to chromosomal region 15F-16F. The mutant alleles were then balanced over an *FM7, Kr>GFP* chromosome. The genomic DNA from homozygous mutant embryos was sequenced for mutations of candidate genes in the region. The sequence of the starting chromosome *y w FRT19A* was used as the reference sequence.

*Immunofluorescence Staining*—Adult females were dissected and ovaries were prepared for immunofluorescence staining according to standard procedures. Third-instar larvae were dissected for imaginal disc staining. The following primary antibodies were used: mouse anti-FasII (catalog no. 1D4, 1:500, DSHB), mouse anti-Cut (catalog no. 2B10, 1:20, DSHB), mouse anti-α-spectrin (catalog no. 3A9, 1:10, DSHB), mouse anti-Dlg (catalog no. 4F3, 1:100, DSHB), mouse anti-Armadillo (catalog no. N2 7A1, 1:100, DSHB), mouse anti-β-gal (catalog no. 40-1a, 1:200, DSHB), mouse anti-Gurken (catalog no. 1D12, 1:10, DSHB), guinea pig anti-Expanded (1:200) (46), guinea pig anti-Merlin (1:200) (47), rabbit anti-atypical PKC (1:1000, Santa Cruz Biotechnology), and rabbit anti-β-spectrin (1:200) (48). Alexa Fluor 647-conjugated secondary antibodies from Invitrogen were used at 1:500. Alexa Fluor 546-phalloidin (1:1000, Invitrogen) and Hoechst (1:10000, Invitrogen) were used to visualize F-actin and DNA, respectively. All images were taken on a Leica TCS SP8 confocal microscope and processed by ImageJ, Adobe Photoshop, and Illustrator.

MCF10A cells were seeded in 6-well plates onto glass coverslips and cultured until the desired density was reached. Cells were then fixed and permeabilized with 4% formaldehyde and 0.1% Triton X-100, respectively. Next, MCF10A cells were blocked using 10% goat serum, followed by incubation with primary and secondary antibodies. The primary antibodies used were mouse YAP antibody (1:100, Santa Cruz Biotechnology) and rabbit polyclonal SPTBN2 antibody (1:100, Proteintech). All images were taken using a Zeiss fluorescence microscope and processed by Adobe software.

*Time-lapse Imaging*—The egg chambers were dissected and cultured for live imaging following the protocol described before (49). All time-lapse imaging was performed on a Leica TCS SP8 confocal microscope using a ×40 water immersion lens with a 488-nm optically pumped semiconductor lasers. Image z stacks were taken at 1-μm steps from the egg chamber surface to 8 μm below the surface. Images were taken at 30-s intervals from 30 min to 2 h.

*S2 Cell Culture, Luciferase Assay, and Quantitative RT-PCR*—S2 cells were cultured at 28 °C in Schneider's *Drosophila* medium (Invitrogen) supplemented with 10% fetal bovine serum and 0.5× penicillin-streptomycin (Invitrogen). S2 cells were seeded in the presence of the indicated dsRNA, followed by transient transfection with the *Yki-pMT*, *Renilla-pMT*, and *3xSd2-Luciferase* plasmids (gifts from Dr. Georg Halder) by Cellfectin II (Invitrogen). After 24 h, copper sulfate was added to a final concentration of 500 μM, and luciferase activity was measured after 3-day incubation using the Promega Dual-Glo kit. The knockdown efficiency for *β-spectrin* was assayed by qRT-PCR.[2] The primer sequences for the *β-spectrin* gene were 5′ACTTCGGTGCGTGCATCTCG3′ and 5′TTGATGCGTTGTCGCTCAGC3′.

*MCF10A Cell Culture, Stable Cell Line Generation, and Confirmation*—MCF10A cells were cultured in DMEM/F12 medium supplemented with horse serum (5%, Sigma), penicillin/streptomycin (1%, Fisher), amphotericin (0.2%, Gemini Bio Products), EGF (20 ng/ml, Novoprotein), hydrocortisone (500 ng/ml, Sigma), insulin (10 μg/ml, Sigma), and cholera toxin (100 ng/ml, Sigma). To generate stable SPTBN2 knockdown cell lines, lentivirus plasmids containing three different *SPTBN2*-targeting shRNA constructs were purchased from Sigma (catalog nos. TRCN0000117127, TRCN0000117128, and TRCN0000117129), and lentiviruses were packaged in HEK293T cells. Virus-containing medium were collected from HEK293T cells 2 days after transfection and used with 2 μg/ml Polybrene to infect MCF10A cells. 1 μg/ml puromycin was used to select infected MCF10A cells for stable cell lines. To confirm SPTBN2 knockdown efficiency in MCF10A cells, the *SPTBN2* mRNA level was tested using qRT-PCR (primer sequences 5′TTTCAACGCCATCGTGCATAA3′ and 5′TGGTCCACATTCACGTCTTCG3′), and SPTBN2 protein was detected by Western blotting using rabbit polyclonal SPTBN2 antibody (1:1000, Proteintech).

## RESULTS

*β-spectrin Mutations in Posterior Follicle Cells (PFCs) Lead to Oocyte Polarity Defects during Mid-oogenesis*—In a *Drosophila* egg chamber, the oocyte resides in a posterior position, surrounded by somatic epithelial follicle cells (FCs). The oocyte establishes the anterior-posterior axis and the dorsal-ventral axis polarity of the egg and embryo during oogenesis (50). The polarization processes are dependent on the interactions between the oocyte and the FCs. In particular, during mid-oogenesis, the oocyte dorsal-ventral asymmetry is established when an unknown signal from the PFCs triggers the oocyte cytoskeleton to repolarize, and then the oocyte nucleus migrates from the posterior end to the future dorsal-anterior corner of the oocyte (50). Multiple signaling pathway activities in the PFCs, including JAK/STAT (40), EGFR (51, 52), Notch (53, 54), and Hippo (55–57), are required for this dorsal-ventral symmetry-breaking event during mid-oogenesis.

In a genetic screen for mutants affecting oocyte polarity (58), a complementation group of six lethal alleles was isolated as required in the PFCs for oocyte dorsal-ventral asymmetry formation. Through recombination and duplication mapping, we mapped the lethality of these alleles to chromosomal region 15F-16F. Sequencing of these alleles showed that they all contained mutations that lead to premature stop codons in the *β-spectrin* gene (Fig. 1*A*). All six alleles exhibited similar phenotypes with comparable severity and penetrance. We therefore used *β-spectrin*$^{FY18}$ as a representative allele for the rest of

[2] The abbreviations used are: qRT-PCR, quantitative RT-PCR; PFC, posterior follicle cell; EGFR, EGF receptor.

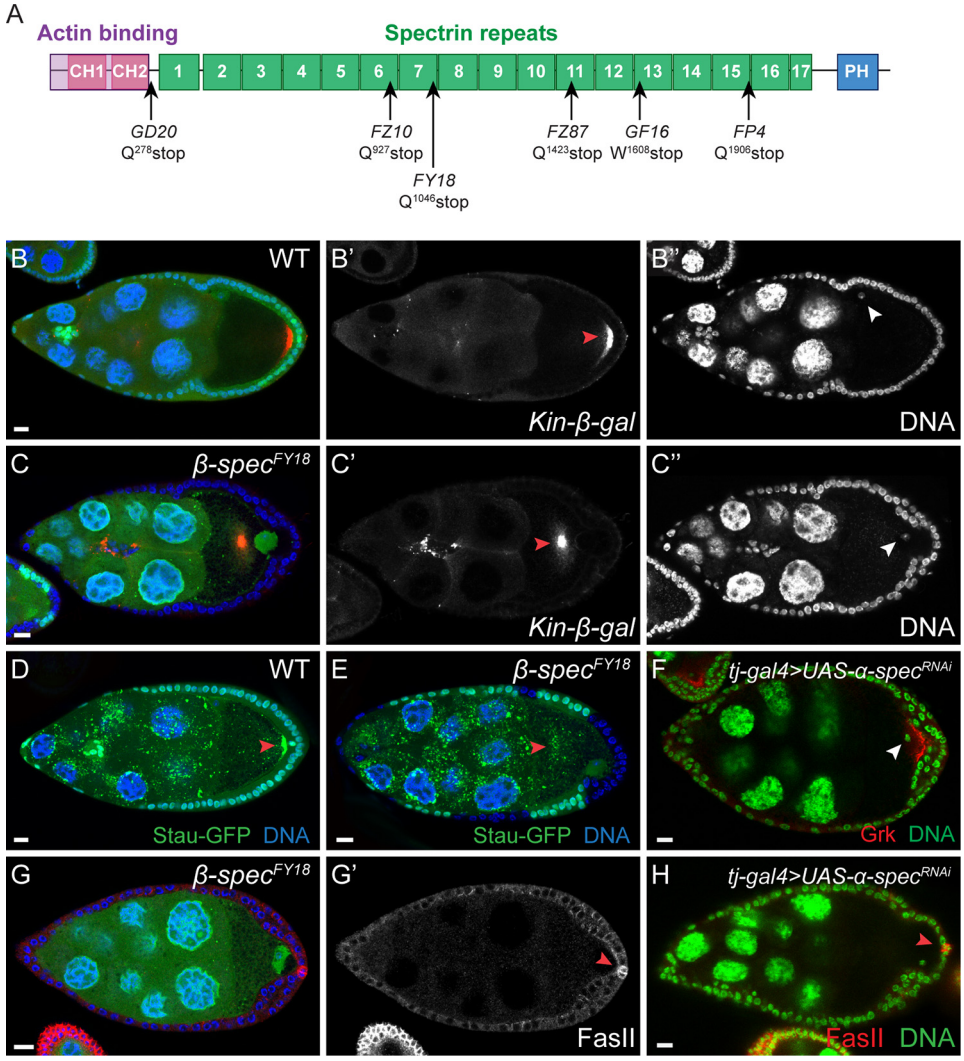


FIGURE 1. **β-spectrin mutations lead to abnormal oocyte polarization.** Follicle cell clones are marked by the absence of GFP (*green*) unless noted otherwise. *Scale bars* = 10 μm unless noted otherwise. *A*, schematic of CG5870, the *Drosophila* β-spectrin protein. All six alleles, including *GD20*, *FZ10*, *FY18*, *FZ87*, *GF16*, and *FP4*, contain premature stop codons at Gln-278, Gln-927, Gln-1046, Gln-1423, Trp-1608, and Gln-1906, respectively. Protein domains are annotated through SMART (75). *CH*, Calponin homology domain; *PH*, pleckstrin homology domain. *B* and *C*, a wild-type egg chamber (*B*) and an egg chamber with *β-spectrin*$^{FY18}$ mutant PFCs (*C*) expressing Kinesin-β-gal are stained for β-gal (*red*) and DNA (*blue*). In the stage 8 wild-type egg chamber, the oocyte nucleus migrates to the dorsal-anterior corner (*B*, *blue*; *B''*, *gray*, *white arrowhead*), and Kinesin-β-gal forms a crescent at the posterior of the oocyte (*B*, *red*; *B'*, *gray*, *red arrowhead*). In the egg chamber containing *β-spectrin*$^{FY18}$ mutant PFCs, the oocyte nucleus stays at the posterior (*C*, *blue*; *C''*, *gray*, *white arrowhead*), and Kinesin-β-gal (*Kin-β-gal)* congregates at the center of the oocyte (*C*, *red*; *C'*, *gray*, *red arrowhead*). *D* and *E*, a wild-type egg chamber (*D*) and an egg chamber with *β-spectrin*$^{FY18}$ mutant PFCs (*E*) expressing Staufen-GFP (*Stau-GFP*, *green*) and stained for DNA (*blue*). In the wild-type egg chamber, Staufen-GFP is tightly localized at the posterior of the oocyte (*red arrowhead*). In the egg chamber containing *β-spectrin*$^{FY18}$ mutant PFCs, Staufen-GFP appears dispersed in the center of the oocyte (*red arrowhead*). *F*, an egg chamber with follicle cells expressing an RNAi construct against *α-spectrin* stained for Gurken (*Grk*, *red*) and DNA (*green*). Note that the oocyte nucleus (*white arrowhead*) stays at the posterior end of the oocyte. Grk is mislocalized at the posterior end of the oocyte together with the oocyte nucleus. *G*, an egg chamber with *β-spectrin*$^{FY18}$ mutant PFCs stained for Fas II (*G*, *red*; *G'*, *gray*) and DNA (*blue*). The posterior polar cells marked by Fas II staining (*red arrowhead*) remain in direct contact with the oocyte, whereas the oocyte polarity is abnormal, marked by the posterior localization of the oocyte nucleus. *H*, an egg chamber with follicle cells expressing an RNAi construct against *α-spectrin* stained for Fas II (*red*) and DNA (*green*). Note that the oocyte remains in direct contact with the posterior polar cells marked by Fas II (*red arrowhead*).

the study. When the PFCs were homozygous mutant for *β-spectrin*, the oocyte nucleus frequently remained at the posterior end of the oocyte during mid-oogenesis (Fig. 1, *B* and *C*, 35.8%, $n = 229$). To confirm that *β-spectrin* mutations lead to a general disruption of oocyte polarity instead of specifically affecting the oocyte nucleus migration event, we further examined a panel of oocyte polarity markers. We first examined a microtubule polarity marker, Kinesin-β-gal. Kinesin-β-gal forms a crescent at the posterior end of the oocyte in a wild-type egg chamber after mid-oogenesis (38) (Fig. 1*B*). Kinesin-β-gal appeared frequently in aggregates or as a diffused cloud in the center of the oocyte in the presence of *β-spectrin* mutant PFCs (Fig. 1*C*, 85.4%, $n = 64$). A second oocyte polarity marker we examined was Staufen. Staufen typically localizes at the posterior end of the oocyte after mid-oogenesis for anchoring the maternal RNAs (59) (Fig. 1*D*). When the PFCs were mutant for *β-spectrin,* Staufen also appeared dispersed in the center of the oocyte (Fig. 1*E*, 91.1%, $n = 90$). Taken together, these results indicate that β-Spectrin is required in the PFCs for the oocyte polarization process during mid-oogenesis.

The *Drosophila* genome contains three spectrin genes, including *α-spectrin* (60), *β-spectrin* (61) and *β-heavy-spectrin*

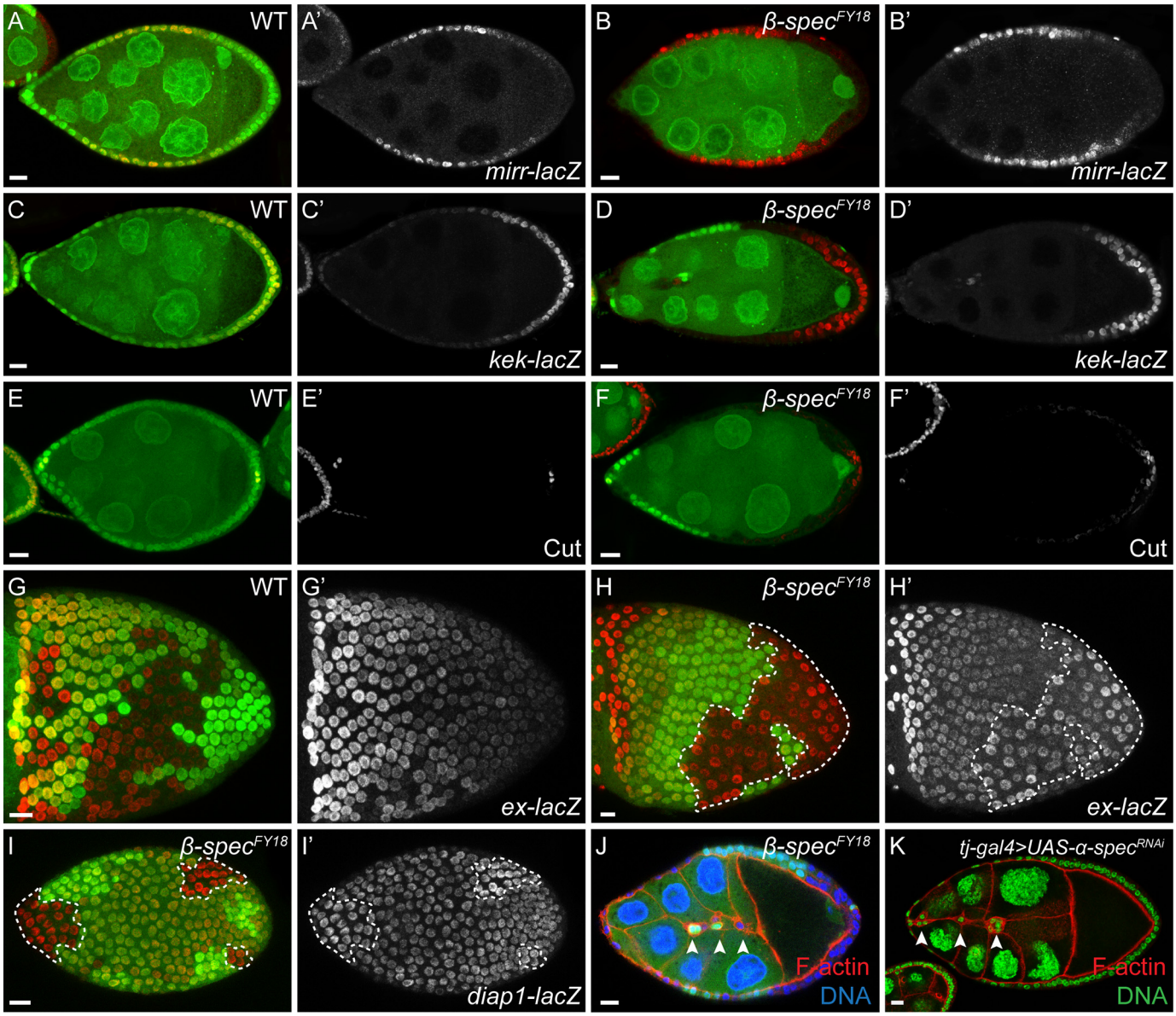


FIGURE 2. **β-spectrin mutations lead to loss of Hippo signaling activity in follicle cells.** Follicle cell clones are marked by the absence of GFP (*green*) unless noted otherwise. *Scale bars* = 10 μm unless noted otherwise. *A* and *B*, the posterior repression of *mirror-lacZ*, a JAK/STAT signaling reporter, is similar in a wild-type egg chamber (*A*, red; *A′*, *gray*) and in an egg chamber containing the *β-spectrin* mutant PFCs (*B*, *red*; *B′*, *gray*). *C* and *D*, the posterior expression pattern of *kekkon-lacZ*, an EGFR signaling reporter, is similar in a wild-type egg chamber (*C*, *red*; *C′*, *gray*) and in an egg chamber where the PFCs are mutant for *β-spectrin* (*D*, *red*; *D′*, *gray*). *E* and *F*, the expression of Cut, a Notch signaling reporter, is down-regulated in a wild-type stage 7/8 egg chamber (*E*, *red*; *E′*, *gray*). The *β-spectrin* mutant PFCs retain Cut expression (*F*, *red*; *F′*, *gray*). *G* and *H*, the expression level of *expanded-lacZ* (*ex-lacZ*), a Hippo signaling reporter, exhibits a gradient pattern from the anterior to the posterior in a wild-type egg chamber (*G*, *red*; *G′*, *gray*). The *β-spectrin* mutant follicle cells show elevated expression levels of *ex-lacZ*, regardless of the clone position (*H*, *red*; *H′*, *gray*; clone boundaries are marked by *dashed lines*). *I*, the *β-spectrin* mutant FCs exhibit elevated expression levels of *diap1-lacZ*, another Hippo signaling reporter (*I*, *red*; *I′*, *gray*; clone boundaries are marked by *dashed lines*). *J*, an egg chamber containing *β-spectrin*$^{FY18}$ mutant border cells stained with phalloidin (*red*) and DNA (*blue*). Border cells fail to migrate as a cluster of cells (*white arrowheads*). *K*, an egg chamber in which *α-spectrin* is depleted in the follicle cells stained with phalloidin (*red*) and DNA (*green*). The border cells fail to migrate as a cluster of cells (*white arrowheads*).

(62). It has been shown previously that *α-spectrin* mutations in the PFCs lead to disruption of oocyte polarity (63). In the report, the authors attributed the oocyte polarity defects to a loss of direct contact between the polar follicle cells and the oocyte, caused by hyperplasia of the *α-spectrin* mutant cells. Although in our experiments 55.9% of the *β-spectrin* mutant PFCs exhibited a hyperplasia phenotype ($n = 228$), a significant portion of the *β-spectrin* mutant cells maintained a monolayered or bilayered epithelial structure even though they exhibited an oocyte polarity defect. When we marked the posterior polar cells with Fas II, in 25 of 27 egg chambers where we observed oocyte polarity defects in the presence of *β-spectrin* mutant PFCs, the posterior polar cells remained in close contact with the oocyte (Fig. 1*G*). Similarly, when we knocked down *α-spectrin* in the follicle cells by RNAi, we observed oocyte polarity defects similar to those in the *β-spectrin* mutants (Fig. 1*F*). Nevertheless, in these cases, the oocyte was frequently observed as being in direct contact with the posterior polar cells (Fig. 1*H*). Therefore, we concluded that the oocyte polarity defects in *β-spectrin* mutants are unlikely to be caused by the separation of the posterior polar cells and the oocyte.

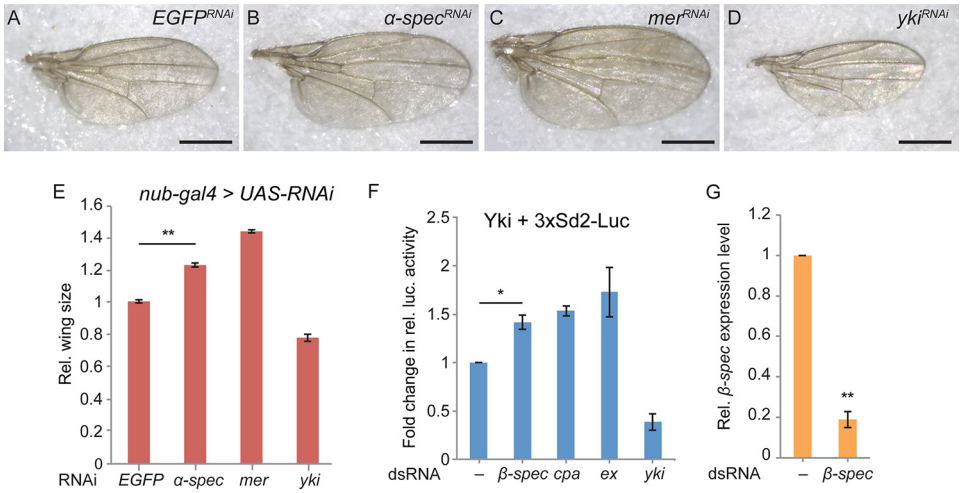


FIGURE 3. **Perturbation of the spectrin network affects adult wing size and Yki activity in S2 cells.** *A–D*, adult wings from flies expressing nub-Gal4 UAS-Dcr2 and UAS-EGFP-RNAi (*A*), UAS-*α-spectrin*-RNAi (*B*), UAS-*mer*-RNAi (*C*), and UAS-*yki*-RNAi (*D*). *Scale bar* = 500 μm. *E*, quantification of the relative (*Rel.*) wing size for each genotype ($n \geq 8$/genotype; **, $p < 0.0001$; Student's *t* test). *F*, a luciferase (*luc.*) reporter assay to measure Yorkie activity in S2 cells. *Drosophila* S2 cells incubated with the indicated dsRNA were transiently transfected with *Yki-pMT*, *Ren-pMT*, and *3xSd2-Luc* plasmids. Luciferase readings are normalized to the *Renilla* luciferase control. Data represent the average of four independent experiments ($n = 4$; *, $p < 0.01$; Student's *t* test). *G*, qRT-PCR analysis of the relative *β-spectrin* transcript levels in the control and *β-spectrin RNAi* cells normalized by *rp49* mRNA level ($n = 3$; **, $p < 0.0001$; Student's *t* test). *Error bars* indicate mean ± S.E.

*β-spectrin Mutations Lead to Loss of Hippo Signaling Activity in Follicle Cells*—The oocyte polarity defects in the presence of *β-spectrin* mutant PFCs suggested that *β-spectrin* mutations might affect one (or more) of the four signaling pathways required in the PFCs for the oocyte polarization process, namely the JAK/STAT, EGFR, Notch, and Hippo signaling pathways. We therefore examined well established signaling reporters for each of these pathways.

First, we examined the expression of *mirror-lacZ (mirr-lacZ)*, a JAK/STAT signaling activity reporter normally repressed in PFCs by JAK/STAT signaling activity during mid-oogenesis (40) (Fig. 2*A*). In the PFCs mutant for *β-spectrin*, the *mirr-lacZ* reporter remained repressed (Fig. 2*B*), indicating that JAK/STAT signaling was not affected in *β-spectrin* mutant PFCs.

Next, we examined the expression of a *kekkon-lacZ (kek-lacZ)* reporter, which is normally induced in PFCs in response to EGFR signaling activation during mid-oogenesis (41) (Fig. 2*C*). The *kek-lacZ* reporter was activated when the PFCs were mutant for *β-spectrin* (Fig. 2*D*), indicating that EGFR signaling was also unaffected by *β-spectrin* mutations.

Notch signaling activity is required for the follicle cells to undergo a mitotic cycle-to-endocycle switch during mid-oogenesis (53, 54). When Notch signaling activity is compromised in follicle cells, the follicle cells continue to divide and fail to differentiate properly along the oocyte anterior-posterior axis. In the presence of loss of function Notch signaling mutant PFCs, oocyte polarity is also disrupted. We therefore examined the expression of Cut, a Notch signaling activity target. Cut expression is normally repressed by Notch signaling activity after stage 6 of oogenesis (Fig. 2*E*) (64). The *β-spectrin* mutant PFCs frequently retained a high level of Cut expression (Fig. 2*F*, 59.3%, $n = 27$). It is noteworthy that *β-spectrin* mutant FCs on the lateral side of the egg chamber did not retain a high Cut expression level (Fig. 2*F*). In other words, *β-spectrin* mutations affected Notch signaling specifically in PFCs, unlike the core Notch signaling pathway mutants, which affect all follicle cells regardless of position along the oocyte anterior-posterior axis. It has been shown previously that such a PFC-specific loss of Notch signaling phenotype is typically exhibited in Hippo pathway mutants (55–57). Therefore, we examined the Hippo signaling activity reporters *expanded-lacZ (ex-lacZ)* (65) and *diap1-lacZ* (66) in follicle cells. Hippo signaling activity normally represses the expression of *expanded-lacZ* (Fig. 2*G*). The *β-spectrin* mutant clones frequently showed elevated expression levels of *ex-lacZ*, regardless of the clone position in the egg chamber (Fig. 2*H*, 67.6%, $n = 37$). Similarly, the expression level of *diap1-lacZ* was also up-regulated in *β-spectrin* mutant cells (Fig. 2*I*, 69.2%, $n = 26$). Moreover, Hippo signaling activity has been shown recently to be required for border cell migration in the follicular epithelium (67). When border cells were mutant for *β-spectrin* (Fig. 2*J*) or when *α-spectrin* was knocked down in border cells by RNAi (Fig. 2*K*), the border cells exhibited migration defects characteristic of those produced by the Hippo pathway mutants. Taken together, our results indicated that *β-spectrin* mutations lead to oocyte polarity defects through disrupting Hippo signaling activity in follicle cells.

To test whether the function of β-Spectrin in the Hippo signaling pathway is specific to the follicular epithelium in *Drosophila*, we first examined spectrin function in the imaginal discs from third-instar larvae. We checked the expression of two Hippo signaling reporters, *cyclin E-lacZ* and *diap1-lacZ* (66), in the eye and wing imaginal discs. We found that the expression level of these reporters in the *β-spectrin* mutant cells was comparable with that of wild-type cells (data not shown), indicating that *β-spectrin* mutations do not significantly affect Hippo signaling activity in the eye and wing imaginal discs. Interestingly, when we knocked down *α-spectrin* in the wing discs through RNAi, we observed a 1.23-fold increase in adult wing size in comparison with the control (Fig. 3, *A–E*), indicating an effect on growth control, most likely via an effect on the Hippo signaling pathway. β-Spectrin is specifically localized to

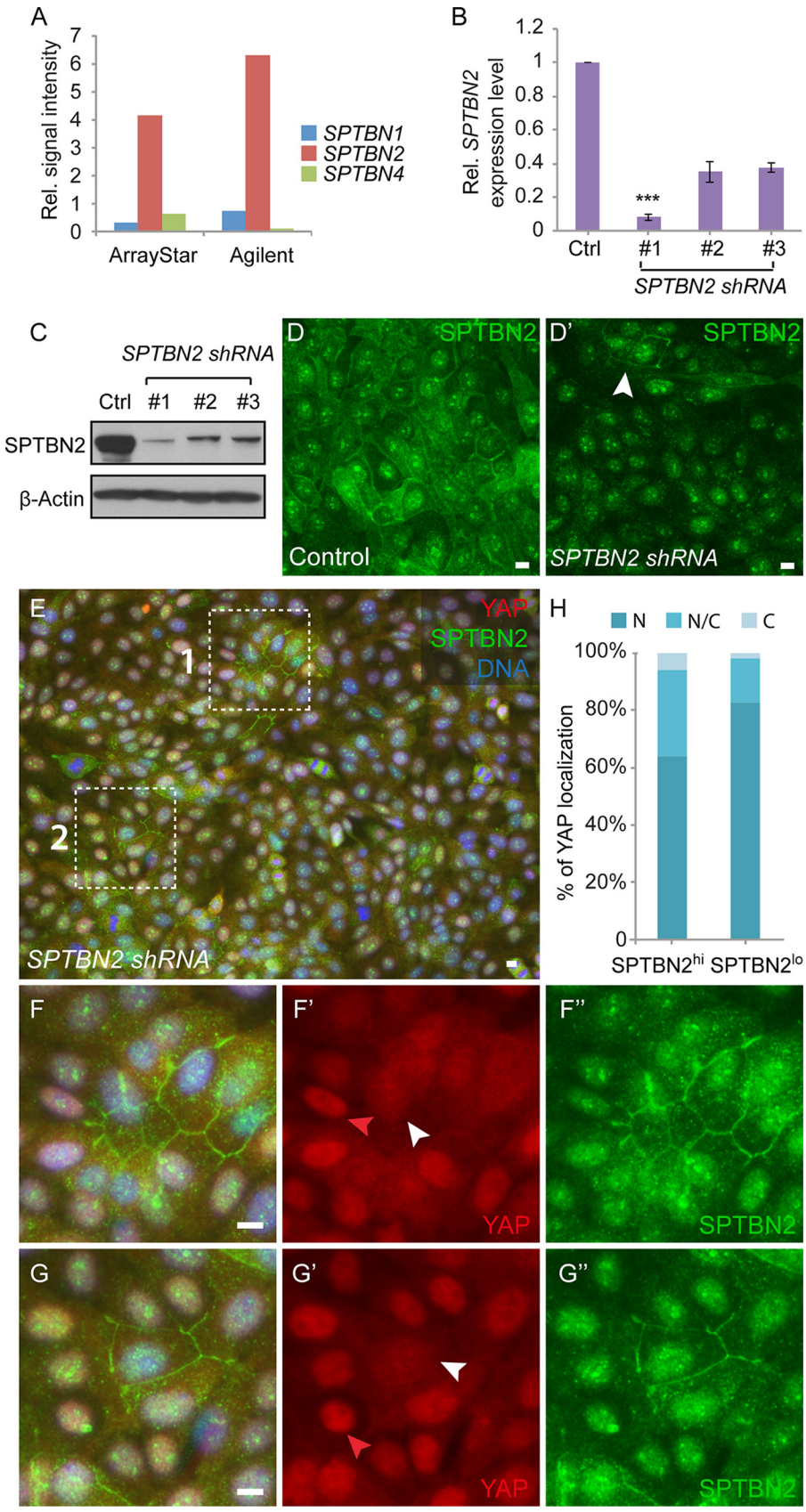
A
Rel. signal intensity
7
6
5
4
3
2
1
0
ArrayStar
Agilent
SPTBN1
SPTBN2
SPTBN4
B
Rel. SPTBN2 expression level
1.2
1
0.8
0.6
0.4
0.2
0
***
Ctrl
#1
#2
#3
SPTBN2 shRNA
C
SPTBN2 shRNA
Ctrl
#1
#2
#3
SPTBN2
β-Actin
D
SPTBN2
Control
D'
SPTBN2
SPTBN2 shRNA
E
YAP
SPTBN2
DNA
1
2
SPTBN2 shRNA
H
N
N/C
C
100%
80%
60%
40%
20%
0
% of YAP localization
SPTBN2hi
SPTBN2lo
F
F'
YAP
F''
SPTBN2
G
G'
YAP
G''
SPTBN2

the lateral domain of epithelial cells, whereas α-Spectrin is localized both apically and laterally (63, 68). Therefore, depletion of α-Spectrin by RNAi might have a stronger effect on the disruption of the spectrin network and Hippo signaling activity in the imaginal disc cells.

In *Drosophila* S2 cells where Yorkie (Yki) was expressed under the control of a *methallothionein* promoter, the luciferase activity of a reporter, 3XSd2-Luc, was used successfully to monitor Yki activity (8). When we treated these cells with dsRNA against *β-spectrin*, we observed a 1.4-fold increase in relative luciferase activity compared with that of the DMSO-treated control group. The increase was comparable with that of the positive control *expanded (ex*) and *capping protein α (cpa*) RNAi (Fig. 3, *F* and *G*). These results indicated that the requirement of β-Spectrin for Hippo signaling activity is not limited to the follicle cells in *Drosophila*.

*β-Spectrin Is Required for Hippo Signaling Activity in Mammalian Cells*—Two recent affinity purification and MS-based proteomic studies have included spectrins in the Hippo pathway protein-protein interaction network (69, 70). Specifically, in cultured human cells, an interaction between the bait protein Salvador homolog 1 (SAV1) and SPTAN1, a human α-Spectrin isoform, has been reported (69). Therefore, we wanted to test whether β-Spectrin has a conserved role in regulating the Hippo pathway in mammals.

We tested the effect of *β-spectrin* knockdown on Hippo signaling activity in human mammary epithelial MCF10A cells. When MCF10A cells are grown at a low cell density, the YAP/TAZ proteins (the mammalian homologs of Yorkie) localize in the cell nucleus and promote proliferation. When MCF10A cell culture reaches a high cell density, the YAP/TAZ proteins translocate to the cytoplasm, and cell proliferation is inhibited (9). In human cells, five genes, *SPTB*, *SPTBN1*, *SPTBN2*, *SPTBN4*, and *SPTBN5*, encode β-spectrins. On the basis of previous studies (71), we focused on SPTBN1, SPTBN2, and SPTBN4, which are most likely to be functional in MCF10A epithelial cells because SPTB and SPTBN5 are known to be more restrictively expressed in neuronal cells and other specific cell types (71). Microarray gene expression profiling of MCF10A cells further demonstrated that *SPTBN2* is most highly expressed among the three *β-spectrin* genes (Fig. 4*A*). Therefore, we chose to knock down SPTBN2 to investigate the potential role of β-spectrin in regulating Hippo signaling activity. MCF10A cells were transduced with lentiviruses containing a scrambled control shRNA construct or three different *SPTBN2*-targeting shRNA constructs, and the knockdown efficiency was confirmed by qRT-PCR (Fig. 4*B*) and Western blotting (Fig. 4*C*). In control cells, SPTBN2 is mostly localized on the cytoplasmic membrane, although the antibody against SPTBN2 also shows nonspecific nucleus staining (Fig. 4*D*). The membrane localization of SPTBN2 was lost in most cells from the *SPTBN2* knockdown population (denoted as $SPTBN2^{lo}$ cells) (Fig. 4*D'*). However, the knockdown was less efficient in a few cells so that they maintained SPTBN2 membrane staining (denoted as $SPTBN2^{hi}$ cells) (Fig. 4*D'*, *arrowhead*). To normalize the effect of local cell density on YAP localization as mentioned previously, we randomly picked clusters of SPTBN2-expressing $SPTBN2^{hi}$ cells in the knockdown population and compared them with their neighboring $SPTBN2^{lo}$ cells. As shown in Fig. 4, *E–H*, compared with $SPTBN2^{lo}$ cells, $SPTBN2^{hi}$ cells showed reduced nuclear localization of YAP, indicating that SPTBN2 regulates YAP localization and activity in MCF10A cells.

*β-spectrin Mutations Lead to Assembly of Abnormal Actin Stress Fibers in the Follicle Cells*—Hippo signaling activity is regulated by a plethora of upstream components, including cell polarity components, cell-cell adhesion molecules, G protein-coupled receptor signaling, and the actin cytoskeleton (2). To understand how β-Spectrin affects Hippo signaling activity, we examined major upstream regulators in *β-spectrin* mutant cells.

β-Spectrin is specifically localized to the lateral domain of the follicle cells (63) (Fig. 5, *A* and *B*). It is possible that β-Spectrin might affect the Hippo signaling pathway through disruption of the cell polarity system. We first examined localization of the cell apical components such as α-Spectrin and aPKC. Both α-Spectrin and aPKC remained apically localized in *β-spectrin* mutant follicle cells (Fig. 5, *C* and *D*). We also examined the apically localized protein Merlin and Expanded, two known upstream regulators of the Hippo signaling pathway. Similarly, the apical localization of Merlin and Expanded remained unchanged in the *β-spectrin* mutant cells (Fig. 5, *E–G*). Next, we examined the adhesion junctional components Ecadherin (Ecad) and Armadillo (Arm, the *Drosophila* β-Catenin homolog). Similarly, the junctional localization of Ecad and Arm was largely unaffected in *β-spectrin* mutant cells (Fig. 5, *H* and *I*). Third, we examined basolateral proteins such as Discs large (Dlg), $Na^+$, and $K^+$-ATPase, and their localization was also unaffected in the *β-spectrin* mutant cells (Fig. 5, *J* and *K*). These results suggest that, although β-Spectrin is part of the cell polarity system, mutations in *β-spectrin* do not disrupt general apical-basal polarity in follicle cells.

Spectrins are well known actin cross-linking proteins (11–13). It is possible that *β-spectrin* mutations might affect the actin cytoskeletal structure in follicle cells. Interestingly, phalloidin staining revealed an abnormal actin cytoskeletal struc-

FIGURE 4. **SPTBN2 is required for Hippo signaling activity in MCF10A cells.** *Scale bars* = 10 μm unless noted otherwise. *A*, microarray analyses of *SPTBN1*, *SPTBN2*, and *SPTBN4* mRNA levels in MCF10A cells using microarray chips from ArrayStar and Agilent. *Rel.*, relative. *B*, qRT-PCR analysis of *SPTBN2* mRNA in *SPTBN2* knockdown MCF10A cells. Stable MCF10A cell lines with *SPTBN2* knockdown were generated using a lentivirus containing three different shRNA constructs. Results were normalized to the *GAPDH* mRNA level. Data represent the average of three independent experiments ($n = 3$; ***, $p < 0.00001$; Student's *t* test). *Error bars* represent mean ± S.E. *Ctrl*, control. *C*, Western blot analysis of MCF10A *SPTBN2* knockdown cells. *D*, MCF10A control (*D*) and *SPTBN2* knockdown cells (*D'*) stained for SPTBN2 (*green*). The SPTBN2 membrane staining is largely absent in the *SPTBN2* knockdown cells (*D'*), except in a few cells (*white arrowhead*, *D'*) where the knockdown efficiency is low. Note that the nucleus signal is nonspecific staining of the primary antibody. *E–G*, MCF10A cells with *SPTBN2* knockdown were stained for YAP (*red*), SPTBN2 (*green*), and DNA (*blue*) (*E*). Regions 1 and 2 (*dashed boxes*) are shown in higher magnification in *F* and *G*, respectively. *Red arrowheads* indicate the nuclear localization of YAP in $SPTBN2^{low}$ cells. *White arrowheads* indicate the nuclear/cytoplasmic localization of YAP in $SPTBN2^{hi}$ cells. *H*, quantification of cytoplasmic (*C*), nuclear and cytoplasmic (*N/C*), or nuclear (*N*) YAP localization in $SPTBN2^{hi}$ cells ($n = 278$) and $SPTBN2^{low}$ cells ($n = 562$).

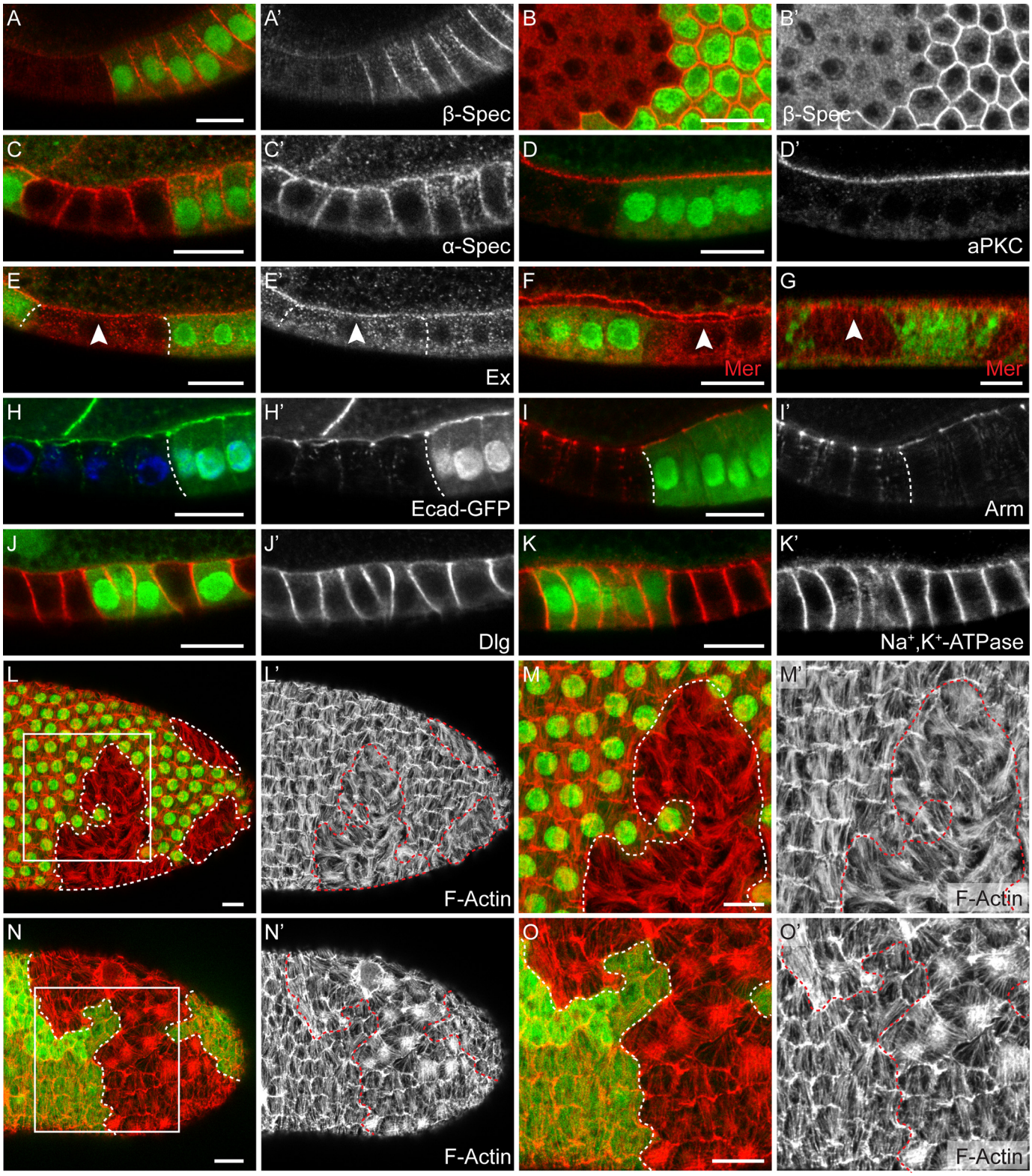


FIGURE 5. **Mutations in *β-spectrin* lead to defects in the actin cytoskeleton network.** Follicle cell and imaginal disc cell clones are marked by the absence of GFP (*green*) unless noted otherwise. *Scale bars* = 10 μm unless noted otherwise. *A* and *B*, FCs stained for β-Spectrin (*β-Spec*; *A* and *B*, *red*; *A'* and *B'*, *gray*). *A*, lateral view. *B*, surface view. β-Spectrin is localized on the lateral side of wild-type cells, and the staining is absent in the *β-spectrin* mutant clones. *C* and *D*, follicle cells stained for α-Spectrin (*C*, *red*; *C'*, *gray*) and aPKC (*D*, *red*; *D'*, *gray*). The apical localization pattern of α-Spectrin and aPKC is unaffected in *β-spectrin* mutant cells. *E–G*, follicle cells (*E* and *F*) and eye imaginal disc cells (*G*) stained for Expanded (*E*, *red*; *E'*, *gray*) and Merlin (*F* and *G*, *red*). Merlin and Expanded remain apically localized in *β-spectrin* mutant cells. *H* and *I*, follicle cells expressing E-cadherin-GFP (*H*, *green*; *H'*, *gray*) and stained for DNA (*H*, *blue*) and follicle cells stained for Armadillo (*Arm*; *I*, *red*; *I'*, *gray*). The junctional localization of E-cadherin and Arm is largely unaffected by *β-spectrin* mutations. *J* and *K*, follicle cells stained for Discs Large (*Dlg*; *J*, *red*; *J'*, *gray*) and $Na^+$ and $K^+$-ATPase (*K*, *red*; *K'*, *gray*). The basolateral localization of Dlg and $Na^+$ and $K^+$-ATPase remains unchanged in *β-spectrin* mutant cells. *L–O*, follicle cells stained with phalloidin to view the basal F-actin network (*L–O*, *red*; *L'–O'*, *gray*). Clone boundaries are marked by *dashed white lines* in *L–O* and *dashed red lines* in *L'–O'*. *M* and *O*, enlarged images from the *boxed regions* in *L* and *N*, respectively. Note that, in the *β-spectrin* mutant cells, the basal F-actin filaments lose the planar polarized parallel bundle structure (*L* and *M*) and often form patches with intensified phalloidin staining (*N* and *O*).

ture on the basal side of *β-spectrin* mutant follicle cells (Fig. 5, *L–O*). The actin filaments on the basal side of wild-type follicle cells are oriented perpendicularly to the anterior-posterior axis of the egg chamber after mid-oogenesis (72). These bundled actin filaments, which are part of the planar cell polarity system in the follicular epithelium, resemble stress fibers in cultured cells. In the *β-spectrin* mutant cells, the actin filaments lose the planar polarized orientation (Fig. 5, *L* and *M*) and frequently form actin patches with intensified phalloidin staining on the basal side of the epithelium (Fig. 5, *N* and *O*). We further analyzed the actin dynamics in the *β-spectrin* mutant cells through time-lapse imaging of cultured live stage 8–9 egg chambers. The F-actin filaments were visualized using an Utrophin-GFP marker (45). Although the basal F-actin filaments appear relatively stable in wild-type follicle cells, as reported previously (supplemental Movie 1) (73), in *β-spectrin* mutant cells, the F-actin filaments failed to assemble into parallel bundles and, instead, initiated radial contractions over time (supplemental Movie 2).

## DISCUSSION

*The Link between the Basal F-actin Phenotype and the Hippo Signaling Defects in β-spectrin Mutant Cells*—Multiple lines of evidence in cultured cells have linked actin stress fibers and YAP/TAZ activity. For example, YAP/TAZ nuclear localization coincided with the presence of abundant stress fibers in cultured cells (5). YAP/TAZ activity decreased in cells treated with the actin depolymerization drugs cytochalasin D and latrunculin A/B, which also reduced stress fiber formation (5, 6). YAP/TAZ activity increased in cultured cells overexpressing Diaphanous, which induced stress fiber formation (4, 8). Several actin binding proteins, including Cofilin 1/2, Capzb, and Gelsolin, were identified as inhibitors of YAP/TAZ activity. Depletion of these proteins caused an increase in both stress fiber formation and YAP/TAZ activity (9).

Follicle cells maintain basal F-actin filaments structurally similar to stress fibers in cultured cells (72). In live *β-spectrin* mutant cells, the F-actin filaments fail to assemble into a planar polarized network and seem to undergo radial contractions, possibly as a result of repeated actin assembly-disassembly cycles. In the fixed *β-spectrin* mutant cells, we observed basal actin patches characterized by intense phalloidin staining and lack of planar polarized organization. In light of previous observations in cell cultures linking the formation of actin stress fibers and YAP/TAZ activity, it seems likely that the basal actin phenotype and the Hippo signaling phenotype in the *β-spectrin* mutant cells are tightly linked.

*Spectrins as General Tension-sensing Molecules underneath the Cell Membrane*—The Hippo signaling pathway is known to link with the cytoskeletal tension in cultured cells (2). Importantly, it has been shown recently that actomyosin-based cellular tension is critical for Hippo signaling activity *in vivo* (10).

Spectrins are long and flexible molecules that form a network underneath the cell membrane. The spectrin function is well characterized in red blood cells as providing cells with mechanical properties, including elasticity and deformability, that allow these cells to survive circulation (74). In other cell types, the spectrin function is much less clear. It has been shown that cytoskeletal tension regulates Hippo activity via promoting Ajuba and Wts complex formation at the adherent junctions in a tension-dependent manner (10). We examined Ajuba and Wts complex localization in follicle cells, and they are both junctionally localized in the *β-spectrin* mutant cells. However, using confocal microscopy, we did not reliably detect a difference of Wts/Ajuba junctional fluorescence intensity between *β-spectrin* mutant cells and wild-type follicle cells (data not shown). It is possible that the spectrin cytoskeleton is part of a cellular tension-sensing system that feeds into the Hippo regulation network. Although we demonstrated a link between spectrin function and actin network organization, a possible link between spectrin function and myosin-based cellular tension still needs further investigation.

*Acknowledgments—We thank Dr. Trudi Schupbach and Dr. Natalie Denef for designing and conducting the original mutant screen and for sharing the β-spectrin mutants. We also thank Dr. Georg Halder, Dr. Richard Fehon, Dr. Christian Klambt, Dr. Lei Zhang, the Bloomington Stock Center, and the Developmental Studies Hybridoma Bank for reagents; Dr. Mingjie Zhang, Dr. Zilong Wen, and Dr. Karl Herrup for sharing confocal microscopes; and Dr. Trudi Schupbach, Dr. Adam Martin, and Dr. Toyotaka Ishibashi for helpful comments on the manuscript.*

## REFERENCES

1. Pan, D. (2010) The hippo signaling pathway in development and cancer. *Dev. Cell* **19,** 491–505
2. Yu, F. X., and Guan, K. L. (2013) The Hippo pathway: regulators and regulations. *Genes Dev.* **27,** 355–371
3. Varelas, X. (2014) The Hippo pathway effectors TAZ and YAP in development, homeostasis and disease. *Development* **141,** 1614–1626
4. Dupont, S., Morsut, L., Aragona, M., Enzo, E., Giulitti, S., Cordenonsi, M., Zanconato, F., Le Digabel, J., Forcato, M., Bicciato, S., Elvassore, N., and Piccolo, S. (2011) Role of YAP/TAZ in mechanotransduction. *Nature* **474,** 179–183
5. Wada, K., Itoga, K., Okano, T., Yonemura, S., and Sasaki, H. (2011) Hippo pathway regulation by cell morphology and stress fibers. *Development* **138,** 3907–3914
6. Zhao, B., Li, L., Wang, L., Wang, C. Y., Yu, J., and Guan, K. L. (2012) Cell detachment activates the Hippo pathway via cytoskeleton reorganization to induce anoikis. *Genes Dev.* **26,** 54–68
7. Fernández, B. G., Gaspar, P., Brás-Pereira, C., Jezowska, B., Rebelo, S. R., and Janody, F. (2011) Actin-capping protein and the Hippo pathway regulate F-actin and tissue growth in *Drosophila*. *Development* **138,** 2337–2346
8. Sansores-Garcia, L., Bossuyt, W., Wada, K., Yonemura, S., Tao, C., Sasaki, H., and Halder, G. (2011) Modulating F-actin organization induces organ growth by affecting the Hippo pathway. *EMBO J.* **30,** 2325–2335
9. Aragona, M., Panciera, T., Manfrin, A., Giulitti, S., Michielin, F., Elvassore, N., Dupont, S., and Piccolo, S. (2013) A mechanical checkpoint controls multicellular growth through YAP/TAZ regulation by actin-processing factors. *Cell* **154,** 1047–1059
10. Rauskolb, C., Sun, S., Sun, G., Pan, Y., and Irvine, K. D. (2014) Cytoskeletal tension inhibits Hippo signaling through an Ajuba-Warts complex. *Cell* **158,** 143–156
11. Pinder, J. C., Bray, D., and Gratzer, W. B. (1975) Actin polymerisation induced by spectrin. *Nature* **258,** 765–766
12. Tilney, L. G., and Detmers, P. (1975) Actin in erythrocyte ghosts and its association with spectrin: evidence for a nonfilamentous form of these two molecules *in situ*. *J. Cell Biol.* **66,** 508–520
13. Cohen, C. M., Tyler, J. M., and Branton, D. (1980) Spectrin-actin associations studied by electron microscopy of shadowed preparations. *Cell* **21,**

875–883
14. Marchesi, V. T., and Steers, E., Jr. (1968) Selective solubilization of a protein component of the red cell membrane. *Science* **159,** 203–204
15. Byers, T. J., and Branton, D. (1985) Visualization of the protein associations in the erythrocyte membrane skeleton. *Proc. Natl. Acad. Sci. U.S.A.* **82,** 6153–6157
16. Tsukita, S., Tsukita, S., and Ishikawa, H. (1980) Cytoskeletal network underlying the human erythrocyte membrane: thin-section electron microscopy. *J. Cell Biol.* **85,** 567–576
17. Palek, J., and Lux, S. E. (1983) Red cell membrane skeletal defects in hereditary and acquired hemolytic anemias. *Semin. Hematol.* **20,** 189–224
18. Agre, P., Casella, J. F., Zinkham, W. H., McMillan, C., and Bennett, V. (1985) Partial deficiency of erythrocyte spectrin in hereditary spherocytosis. *Nature* **314,** 380–383
19. Agre, P., Orringer, E. P., and Bennett, V. (1982) Deficient red-cell spectrin in severe, recessively inherited spherocytosis. *New Engl. J. Med.* **306,** 1155–1161
20. Mohandas, N., and Gallagher, P. G. (2008) Red cell membrane: past, present, and future. *Blood* **112,** 3939–3948
21. Bennett, V., Davis, J., and Fowler, W. E. (1982) Brain spectrin, a membrane-associated protein related in structure and function to erythrocyte spectrin. *Nature* **299,** 126–131
22. Burridge, K., Kelly, T., and Mangeat, P. (1982) Nonerythrocyte spectrins: actin-membrane attachment proteins occurring in many cell types. *J. Cell Biol.* **95,** 478–486
23. Glenney, J. R., Jr., Glenney, P., Osborn, M., and Weber, K. (1982) An F-actin- and calmodulin-binding protein from isolated intestinal brush borders has a morphology related to spectrin. *Cell* **28,** 843–854
24. Bennett, V., and Baines, A. J. (2001) Spectrin and ankyrin-based pathways: metazoan inventions for integrating cells into tissues. *Physiol. Rev.* **81,** 1353–1392
25. Nelson, W. J., Shore, E. M., Wang, A. Z., and Hammerton, R. W. (1990) Identification of a membrane-cytoskeletal complex containing the cell adhesion molecule uvomorulin (E-cadherin), ankyrin, and fodrin in Madin-Darby canine kidney epithelial cells. *J. Cell Biol.* **110,** 349–357
26. Lee, J. K., Coyne, R. S., Dubreuil, R. R., Goldstein, L. S., and Branton, D. (1993) Cell shape and interaction defects in alpha-spectrin mutants of *Drosophila melanogaster*. *J. Cell Biol.* **123,** 1797–1809
27. McKeown, C., Praitis, V., and Austin, J. (1998) sma-1 encodes a βH-spectrin homolog required for *Caenorhabditis elegans* morphogenesis. *Development* **125,** 2087–2098
28. Mangeat, P. H., and Burridge, K. (1984) Immunoprecipitation of nonerythrocyte spectrin within live cells following microinjection of specific antibodies: relation to cytoskeletal structures. *J. Cell Biol.* **98,** 1363–1377
29. Hammarlund, M., Davis, W. S., and Jorgensen, E. M. (2000) Mutations in β-spectrin disrupt axon outgrowth and sarcomere structure. *J. Cell Biol.* **149,** 931–942
30. Moorthy, S., Chen, L., and Bennett, V. (2000) *Caenorhabditis elegans* β-G spectrin is dispensable for establishment of epithelial polarity, but essential for muscular and neuronal function. *J. Cell Biol.* **149,** 915–930
31. Gao, Y., Perkins, E. M., Clarkson, Y. L., Tobia, S., Lyndon, A. R., Jackson, M., and Rothstein, J. D. (2011) β-III spectrin is critical for development of Purkinje cell dendritic tree and spine morphogenesis. *J. Neurosci.* **31,** 16581–16590
32. Featherstone, D. E., Davis, W. S., Dubreuil, R. R., and Broadie, K. (2001) *Drosophila* α- and β-spectrin mutations disrupt presynaptic neurotransmitter release. *J. Neurosci.* **21,** 4215–4224
33. Pielage, J., Fetter, R. D., and Davis, G. W. (2005) Presynaptic spectrin is essential for synapse stabilization. *Curr. Biol.* **15,** 918–928
34. Pielage, J., Fetter, R. D., and Davis, G. W. (2006) A postsynaptic spectrin scaffold defines active zone size, spacing, and efficacy at the *Drosophila* neuromuscular junction. *J. Cell Biol.* **175,** 491–503
35. Xu, K., Zhong, G., and Zhuang, X. (2013) Actin, spectrin, and associated proteins form a periodic cytoskeletal structure in axons. *Science* **339,** 452–456
36. Krieg, M., Dunn, A. R., and Goodman, M. B. (2014) Mechanical control of the sense of touch by β-spectrin. *Nat. Cell Biol.* **16,** 224–233
37. Denef, N., Chen, Y., Weeks, S. D., Barcelo, G., and Schüpbach, T. (2008) Crag regulates epithelial architecture and polarized deposition of basement membrane proteins in *Drosophila*. *Dev. Cell* **14,** 354–364
38. Clark, I., Giniger, E., Ruohola-Baker, H., Jan, L. Y., and Jan, Y. N. (1994) Transient posterior localization of a kinesin fusion protein reflects anteroposterior polarity of the *Drosophila* oocyte. *Curr. Biol.* **4,** 289–300
39. Schuldt, A. J., Adams, J. H., Davidson, C. M., Micklem, D. R., Haseloff, J., St Johnston, D., and Brand, A. H. (1998) Miranda mediates asymmetric protein and RNA localization in the developing nervous system. *Genes Dev.* **12,** 1847–1857
40. Xi, R., McGregor, J. R., and Harrison, D. A. (2003) A gradient of JAK pathway activity patterns the anterior-posterior axis of the follicular epithelium. *Dev. Cell* **4,** 167–177
41. Pai, L. M., Barcelo, G., and Schüpbach, T. (2000) D-cbl, a negative regulator of the Egfr pathway, is required for dorsoventral patterning in *Drosophila* oogenesis. *Cell* **103,** 51–61
42. Boedigheimer, M., and Laughon, A. (1993) Expanded: a gene involved in the control of cell proliferation in imaginal discs. *Development* **118,** 1291–1301
43. Hay, B. A., Wassarman, D. A., and Rubin, G. M. (1995) *Drosophila* homologs of baculovirus inhibitor of apoptosis proteins function to block cell death. *Cell* **83,** 1253–1262
44. Oda, H., and Tsukita, S. (2001) Real-time imaging of cell-cell adherens junctions reveals that *Drosophila* mesoderm invagination begins with two phases of apical constriction of cells. *J. Cell Sci.* **114,** 493–501
45. Rauzi, M., Lenne, P. F., and Lecuit, T. (2010) Planar polarized actomyosin contractile flows control epithelial junction remodelling. *Nature* **468,** 1110–1114
46. Maitra, S., Kulikauskas, R. M., Gavilan, H., and Fehon, R. G. (2006) The tumor suppressors Merlin and Expanded function cooperatively to modulate receptor endocytosis and signaling. *Curr. Biol.* **16,** 702–709
47. McCartney, B. M., and Fehon, R. G. (1996) Distinct cellular and subcellular patterns of expression imply distinct functions for the *Drosophila* homologues of moesin and the neurofibromatosis 2 tumor suppressor, merlin. *J. Cell Biol.* **133,** 843–852
48. Hülsmeier, J., Pielage, J., Rickert, C., Technau, G. M., Klämbt, C., and Stork, T. (2007) Distinct functions of α-Spectrin and β-Spectrin during axonal pathfinding. *Development* **134,** 713–722
49. Prasad, M., Jang, A. C., Starz-Gaiano, M., Melani, M., and Montell, D. J. (2007) A protocol for culturing *Drosophila* melanogaster stage 9 egg chambers for live imaging. *Nat. Protoc.* **2,** 2467–2473
50. Roth, S., and Lynch, J. A. (2009) Symmetry breaking during *Drosophila* oogenesis. *Cold Spring Harb. Perspect. Biol.* **1,** a001891
51. González-Reyes, A., Elliott, H., and St Johnston, D. (1995) Polarization of both major body axes in *Drosophila* by gurken-torpedo signalling. *Nature* **375,** 654–658
52. Roth, S., Neuman-Silberberg, F. S., Barcelo, G., and Schüpbach, T. (1995) cornichon and the EGF receptor signaling process are necessary for both anterior-posterior and dorsal-ventral pattern formation in *Drosophila*. *Cell* **81,** 967–978
53. Deng, W. M., Althauser, C., and Ruohola-Baker, H. (2001) Notch-Delta signaling induces a transition from mitotic cell cycle to endocycle in *Drosophila* follicle cells. *Development* **128,** 4737–4746
54. López-Schier, H., and St Johnston, D. (2001) Delta signaling from the germ line controls the proliferation and differentiation of the somatic follicle cells during *Drosophila* oogenesis. *Genes Dev.* **15,** 1393–1405
55. Meignin, C., Alvarez-Garcia, I., Davis, I., and Palacios, I. M. (2007) The salvador-warts-hippo pathway is required for epithelial proliferation and axis specification in *Drosophila*. *Curr. Biol.* **17,** 1871–1878
56. Polesello, C., and Tapon, N. (2007) Salvador-warts-hippo signaling promotes *Drosophila* posterior follicle cell maturation downstream of notch. *Curr. Biol.* **17,** 1864–1870
57. Yu, J., Poulton, J., Huang, Y. C., and Deng, W. M. (2008) The hippo pathway promotes Notch signaling in regulation of cell differentiation, proliferation, and oocyte polarity. *PLoS ONE* **3,** e1761
58. Yan, Y., Denef, N., Tang, C., and Schüpbach, T. (2011) *Drosophila* PI4KIIIα is required in follicle cells for oocyte polarization and Hippo signaling. *Development* **138,** 1697–1703
59. St Johnston, D., Beuchle, D., and Nüsslein-Volhard, C. (1991) Staufen, a

gene required to localize maternal RNAs in the *Drosophila* egg. *Cell* **66,** 51–63
60. Byers, T. J., Dubreuil, R., Branton, D., Kiehart, D. P., and Goldstein, L. S. (1987) *Drosophila* spectrin: II: conserved features of the α-subunit are revealed by analysis of cDNA clones and fusion proteins. *J. Cell Biol.* **105,** 2103–2110
61. Byers, T. J., Husain-Chishti, A., Dubreuil, R. R., Branton, D., and Goldstein, L. S. (1989) Sequence similarity of the amino-terminal domain of *Drosophila* β spectrin to α actinin and dystrophin. *J. Cell Biol.* **109,** 1633–1641
62. Dubreuil, R. R., Byers, T. J., Stewart, C. T., and Kiehart, D. P. (1990) A β-spectrin isoform from *Drosophila* (β H) is similar in size to vertebrate dystrophin. *J. Cell Biol.* **111,** 1849–1858
63. Lee, J. K., Brandin, E., Branton, D., and Goldstein, L. S. (1997) α-Spectrin is required for ovarian follicle monolayer integrity in *Drosophila melanogaster*. *Development* **124,** 353–362
64. Sun, J., and Deng, W. M. (2005) Notch-dependent downregulation of the homeodomain gene cut is required for the mitotic cycle/endocycle switch and cell differentiation in *Drosophila* follicle cells. *Development* **132,** 4299–4308
65. Hamaratoglu, F., Willecke, M., Kango-Singh, M., Nolo, R., Hyun, E., Tao, C., Jafar-Nejad, H., and Halder, G. (2006) The tumour-suppressor genes NF2/Merlin and Expanded act through Hippo signalling to regulate cell proliferation and apoptosis. *Nat. Cell Biol.* **8,** 27–36
66. Harvey, K. F., Pfleger, C. M., and Hariharan, I. K. (2003) The *Drosophila* Mst ortholog, hippo, restricts growth and cell proliferation and promotes apoptosis. *Cell* **114,** 457–467
67. Lucas, E. P., Khanal, I., Gaspar, P., Fletcher, G. C., Polesello, C., Tapon, N., and Thompson, B. J. (2013) The Hippo pathway polarizes the actin cytoskeleton during collective migration of *Drosophila* border cells. *J. Cell Biol.* **201,** 875–885
68. Pesacreta, T. C., Byers, T. J., Dubreuil, R., Kiehart, D. P., and Branton, D. (1989) *Drosophila* spectrin: the membrane skeleton during embryogenesis. *J. Cell Biol.* **108,** 1697–1709
69. Couzens, A. L., Knight, J. D., Kean, M. J., Teo, G., Weiss, A., Dunham, W. H., Lin, Z. Y., Bagshaw, R. D., Sicheri, F., Pawson, T., Wrana, J. L., Choi, H., and Gingras, A. C. (2013) Protein interaction network of the mammalian Hippo pathway reveals mechanisms of kinase-phosphatase interactions. *Sci. Signal.* **6,** rs15
70. Kwon, Y., Vinayagam, A., Sun, X., Dephoure, N., Gygi, S. P., Hong, P., and Perrimon, N. (2013) The Hippo signaling pathway interactome. *Science* **342,** 737–740
71. Machnicka, B., Grochowalska, R., Bogusławska, D. M., Sikorski, A. F., and Lecomte, M. C. (2012) Spectrin-based skeleton as an actor in cell signaling. *Cell. Mol. Life Sci.* **69,** 191–201
72. Gutzeit, H. O. (1990) The microfilament pattern in the somatic follicle cells of mid-vitellogenic ovarian follicles of *Drosophila*. *Eur. J. Cell Biol.* **53,** 349–356
73. He, L., Wang, X., Tang, H. L., and Montell, D. J. (2010) Tissue elongation requires oscillating contractions of a basal actomyosin network. *Nat. Cell Biol.* **12,** 1133–1142
74. Delaunay, J. (2007) The molecular basis of hereditary red cell membrane disorders. *Blood Rev.* **21,** 1–20
75. Schultz, J., Milpetz, F., Bork, P., and Ponting, C. P. (1998) SMART, a simple modular architecture research tool: identification of signaling domains. *Proc. Natl. Acad. Sci. U.S.A.* **95,** 5857–5864